pharmaceutics

MDPI

Article

Pulmonary delivery of curcumin and beclomethasone dipropionate in a multicomponent nanosuspension for the treatment of bronchial asthma

Luca Casula [1], Francesco Lai [1], Elena Pini [2], Donatella Valenti [1], Chiara Sinico [1], Maria Cristina Cardia [1], Salvatore Marceddu [3], Giorgia Ailuno [4] and Anna Maria Fadda [1,*]

[1] Dipartimento di Scienze della Vita e dell'Ambiente, Sezione di Scienze del Farmaco, Università degli Studi di Cagliari, 09124 Cagliari, Italy; luca.casula@unica.it (L.C.); frlai@unica.it (F.L.); valenti@unica.it (D.V.); sinico@unica.it (C.S.); cardiamr@unica.it (M.C.C.); mfadda@unica.it (A.M.F.)
[2] DISFARM, Sezione di Chimica Generale e Organica "A. Marchesini", Università degli Studi di Milano, Via Venezian 21, 20133 Milano, Italy; elena.pini@unimi.it (E.P.)
[3] Istituto di Scienze delle Produzioni Alimentari (ISPA)-CNR, Sez. di Sassari, 07040 Baldinca, Italy; salvatore.marceddu@cnr.it (S.M.)
[4] Department of Pharmacy, University of Genova, Genova, 16147, Italy; ailuno@difar.unige.it (G.A.)
* Correspondence: mfadda@unica.it; Tel.: +39-070-675-8565

Abstract: Curcumin has shown an extraordinary efficacy as an add-on ingredient in asthma treatment, due to its immunomodulatory and anti-inflammatory activity. However, its low water solubility and bioavailability lead to a poor therapeutic effect, which can be overcome by its formulation as nanocrystals. The aim of this study was to prepare a multicomponent formulation for the delivery of curcumin (CUR) and beclomethasone dipropionate (BDP) into the lungs as water-based nanosuspensions (NS). Single component formulations (CUR-NS, BDP-NS) and a multi-component formulation (CUR+BDP-NS) were prepared through a wet ball media milling technique, using P188 as a non-toxic stabilizer. Characterization was carried out in terms of size, size distribution, zeta potential, nanocrystals morphology and solid-state properties. Moreover, the inhalation delivery efficiency was studied with Next Generation Impactor (NGI, Apparatus E Ph. Eu). CUR-NS was optimized and showed a long-term stability and improved nanocrystals solubility. The three formulations exhibited a nanocrystal mean diameter in the range 200-240 nm and a homogenous particle size distribution. Aggregation or sedimentation phenomena were not observed in the multicomponent formulation on 90 days storage at room temperature. Finally, the nebulization tests of the three samples showed optimal aerodynamic parameters and MMAD < 5 μm.

Keywords: curcumin, beclomethasone dipropionate, nanosuspension, asthma, pulmonary delivery, NGI, DSC, XRPD, ATR-FTIR

Citation: Lastname, F.; Lastname, F.; Lastname, F. Title. *Pharmaceutics* **2021**, *13*, x. https://doi.org/10.3390/xxxxx

Academic Editor: Firstname Lastname

Received: date
Accepted: date
Published: date

1. Introduction

Bronchial asthma is a chronic inflammatory disease, characterized by a complex interplay of airway inflammation and hyper-responsiveness, reversible airway obstruction, mucus hypersecretion and pulmonary edema. The main common symptoms include cough, chest tightness, dyspnea and wheezing [1,2]. The well-known 'umbrella' asthma diagnosis helps to describe the heterogeneity of the disease and to identify the involved endotypes and phenotypes [3]. In particular, the prevalent phenotypes can be classified as: early-onset allergic, late-onset eosinophilic, exercise-induced, obesity-related and neutrophilic [4]. As regards the pathogenesis of asthma, the disease development is associated with the expression of several transcription factors and in particular the Nuclear Factor- κB (NF-κB), [5]. Medications for the long-term treatment of asthma can be classified

into: (i) controller medications, to control the symptoms and reduce exacerbations, (ii) reliever/rescue medications, to provide an immediate relief of breakthrough symptoms, and (iii) add-on therapies for patients with severe asthma. Treatment includes inhaled corticosteroids (CS), long-acting beta2-agonist (LABA), leukotriene receptor antagonist (LTRA), oral corticosteroids (OCS) and short-acting beta2-agonist (SABA) [6]. In the recent years, an increasing interest in complementary and alternative treatments in asthma patients has been shown. Natural extracts, also known as herbal medicinal products, are the most used complementary products or health-promoting agents, due to their health benefits and reduced side effects [7]. Among others, curcumin, a polyphenol extracted from the rhizome of Curcuma longa, has shown a potential therapeutic value and promising pharmacological activities in a variety of chronic diseases, including bronchial asthma [8]. Its antioxidant and anti-inflammatory activities act synergically to stop the inflammatory process. In particular, curcumin ability to attenuate airway inflammation seems to be due to the inhibition of NF-kB in the asthmatic lung tissue, which is highly involved in the pathogenesis of the disease [9,10]. Moreover, levels of pro-inflammatory and pro-fibrotic cytokines, chemokines and heat shock proteins were found to be reduced by the polyphenol action, whereas aquaporin expression increased, leading to reduction of pulmonary oedema [11]. However, the low aqueous solubility is limiting for its potential therapeutic applications. A possible strategy to improve the pulmonary delivery of curcumin might be its administration as nanocrystals [12]. Nanocrystals are nanoparticles of pure drug without any matrix material, suspended in an outer liquid phase, usually composed of water and/or water-miscible solvents, and stabilized using an ionic or non-ionic surfactant or polymers [13]. The drug nanocrystals average diameter is below 1 μm (typically in the range of 200-500 nm). Due to the increased particle surface area and the decreased diffusion layer thickness (compared to coarse and micronized drugs), the dissolution rate is sped up, as described by the Prandtl equation [14]. The Freundlich–Ostwald equation shows that nanocrystals are also characterized by an enhanced saturation solubility [15]. Furthermore, poorly soluble drugs for lung delivery have shown to have superior pharmacokinetics properties when formulated as nanocrystals, compared to solutions or coarse suspensions of the same drug [16–21]. Therefore, the aim of our work was to formulate a multi-component nanocrystal suspension for the inhalation therapy, composed of beclomethasone dipropionate – corticosteroid agent, well-known for its activity to reduce the symptoms [6,22] – and curcumin as natural complementary agent. At first, curcumin nanosuspension (CUR-NS) was prepared by a top down - media milling method [23]. The multi component nanosuspension (CUR+BDP-NS) was then prepared using a beclomethasone dipropionate nanosuspension (BDP-NS) studied in our previous work [24]. Characterization of the nanosuspensions was carried out via different techniques: dynamic light scattering (DLS), scanning electron microscopy (SEM), differential scanning calorimetry (DSC), X-ray powder diffractometry (XRPD) and Attenuated Total Reflectance-Fourier Transform Infrared (ATR-FTIR) spectroscopy. Finally, nebulization tests with Next Generation Impactor (NGI, Apparatus E Ph. Eu) were carried out to study the aerodynamic properties of the obtained formulations.

2. Materials and Methods

2.1. Materials

Beclomethasone dipropionate, curcumin, Kolliphor P188 (Poloxamer 188, P188) were obtained from Sigma Aldrich (Italy). All the other products were of analytical grade. he

2.2. Preparation of nanosuspension

The nanosuspensions were prepared through a wet ball media milling technique, using a 2:1 (w/w) drug:stabilizer ratio. The drug was dispersed in a (0.5 and 1%, w/w) Poloxamer 188 (P188) water solution using an Ultra Turrax T25 basic (IKA, Werke) for 6 min at

8000 rpm. This coarse suspension was divided in 1.5 ml conical microtubes containing about 0.4 g of 0.1-0.2 mm yttrium-stabilized zirconia-silica beads (Silibeads® Typ ZY Sigmund Lindner, Germany). For the CUR-NS, the microtubes were oscillated at 3000 rpm for 70 minutes using a beads-milling cell disruptor equipment (Disruptor Genie®, Scientific Industries, USA). The obtained nanosuspensions of each microtube were gathered and then separated from the milling beads by sieving. As concerns the BDP-NS, the formulation was prepared as previously reported [24]. The procedure was the same as for the CUR-NS, and the oscillation time of the microtubes at 3000 rpm was 150 minutes. The formulations had a final concentration of 1% (w/w) active compound (CUR or BDP) and 0.5% (w/w) P188.

2.3. Particle size analysis

Average diameter and polydispersity index (PDI, as a measure of the size distribution width) of the samples were determined by Dynamic Light Scattering (DLS) using a Zetasizer nano (Malvern Instrument, Worcestershire, United Kingdom). Samples were backscattered by a helium–neon laser (633 nm) at an angle of 173° and a constant temperature of 25°C. Zeta potential was estimated using the Zetasizer nano by means of the M3-PALS (Phase Analysis Light Scattering) technique. Just before the analysis, nanosuspensions were diluted with distilled water. Furthermore, a medium-term stability study of the CUR nanosuspension stored at room temperature was performed by monitoring average size, polydispersity index, and zeta potential for 90 days. All the measurements were made in triplicate.

2.4. Scanning electron microscopy

In order to investigate the (nano)crystals morphology, CUR raw powder and CUR-NS were analysed through a Zeiss ESEM EVO LS 10 (Germany) environmental scanning electron microscope (SEM), operating at 20 KV in high vacuum modality with secondary electron detector (SEI). For the CUR raw powder, the sample was mounted on an aluminium stub with carbon adhesive discs and coated with gold in an Agar Automatic Sputter Coater B7341. As regards the CUR-NS, a drop of the sample was firstly placed on a glass slide and air dried, and then mounted on the stub following the procedure stated above.

2.5. Solubility studies

CUR solubility in water was measured for the CUR bulk powder and CUR-NS. The formulations (n = 3) were kept under constant stirring for 72 h at 37°C. Samples were withdrawn and centrifuged at 15,000 rpm for 60 min; the supernatant was centrifuged again at 15,000 rpm for 60 min. Then, a known amount of the clear supernatant was withdrawn and diluted with methanol for the HPLC analysis.

2.6. Solid state characterization

CUR, BDP, P188, physical mixtures of CUR:P188 and BDP:P188 in amounts equivalent to the ratios present in the formulations, and the two single-component formulations (CUR-NS and BDP-NS) were investigated by using different technologies such as DSC, XRPD, and ATR-FTIR spectroscopy.

DSC analysis (Perkin Elmer DSC 6 Waltham, MA, USA) was used to characterize the thermal behaviour of the different components used for the formulations. Samples were hermetically sealed in an aluminium pan and heated at a speed of 10 mL/min in the range between 30 and 220°C. Inert atmosphere was maintained by purging nitrogen at a flow rate of 10 mL/min. A control empty pan subjected to the same heating conditions was used as a reference.

ATR-FT-IR spectra were acquired with a Perkin Elmer Spectrum One FT-IR (Perkin Elmer, Waltham, MA, USA), equipped with a Perkin Elmer Universal ATR sampling accessory consisting of a diamond crystal. Analyses were performed in a spectral region

between 4000 and 650 cm-1 and analysed by transmittance technique with 32 scansions and 4 cm-1 resolution.

XRPD patterns were collected with a Rigaku MiniFlex diffractometer, operating at 30 kV and at 15 mA, with Cu Kα radiation (1.54056 Å) in the range from 3 to 60 2θ, in steps of 0.02, using a scan step time of 2.00 seconds. The results were then obtained as peak height (intensity) versus 2θ.

2.7. Preparation of nanosuspension

CUR-NS and BDP-NS were prepared as described above (2.2). The multicomponent nanosuspension (CUR+BDP-NS) was prepared right before the nebulization test by mixing equal parts of CUR-NS and BDP-NS. The formulation was adequately vortexed and then visually inspected to check the absence of large precipitated aggregates or phase separation. Finally, particle size analysis was carried out by DLS.

2.8. Nebulization and aerodynamic behaviour of nanosuspensions

CUR-NS, BDP-NS and CUR+BDP-NS were nebulized using a Pari SX® air jet nebulizer attached to a Pari TurboBoy® compressor (Pari GmnH, Starnberg, Germany) and connected to the Next Generation Impactor (NGI, Apparatus E, Eur. Ph 7.2, Copley Scientific Ltd., Nottingham, United Kingdom). All the parts of the NGI were washed in methanol and allowed to dry. The collection plates were not sprayed with silicone fluid in accordance with the European Pharmaceutical Aerosol Group (EPAG) recommendations [25]. Pre-separator, which is mostly indicated for dry powder inhalers to separate very large particles and avoid blockage of NGI stages, was not used during this study.

The formulation (2 ml) was placed in the nebulizer and aerosolized to dryness directly into the throat of the NGI, using a flow rate of 15 L/min [26]. At the end of the experiment, the drug amount deposited in each stage of the impactor and the residual (undelivered) was collected, using methanol, in a glass vial, properly diluted and analysed by HPLC. The following nebulization parameters were evaluated: (1) the Emitted Dose (ED%), calculated as the percentage of drug recovered in the NGI versus the amount of drug placed in the nebulizer; (2) the Fine Particle Dose (FPD), which represents the amount of drug contained in droplets of size less than 5 μm; and (3) the Fine Particle Fraction (FPF%), calculated as percentage of FPD versus the amount of drug recovered in the NGI.

The cumulative amount of drug-containing droplets with a diameter lower than the stated size of each stage was plotted as a percentage of the recovered drug versus the cut-off diameter, not including the mass deposited in the induction port due to the unavailability of a precise upper size limit for particles deposited in this section [27]. Finally, the Mass median aerodynamic diameter (MMAD) of the particles was extrapolated from the graph according to the Eur. Ph. 7.2, and the geometric standard deviation (GSD) value was calculated.

2.9. HPLC analysis

Quantitative determination of BDP and CUR was performed by HPLC using a liquid chromatograph Alliance 2690 (Waters Corp, Milford, MA) equipped with a photodiode array detector and a computer integrating apparatus (Empower 3). Analyses were performed with a Sunfire C18 column (3.5 μm, 4.6 mm × 150 mm, Waters). The mobile phase was a mixture of acetonitrile, water and acetic acid (95:4.84:0.16 v/v), delivered at a flow rate of 0.5 mL/min. Samples (10μL) were injected using an auto sampler. CUR was revealed at 421 nm, whereas BDP at 240 nm. The stock standard solutions of CUR and BDP were prepared by dissolving the drug in methanol and stored at 4 °C. A standard calibration curve (peak area of CUR/BDP vs. known drug concentration) was built up by using standard solutions prepared by dilution of the stock standard solution with the mobile phase. Calibration graphs were plotted according to the linear regression analysis, which

gave a correlation coefficient value (R2) of 0.999. The limit of quantification was 10 ng for CUR and 5 ng for BDP, while the limit of detection was 2 ng for both compounds. Sample preparation and analyses were performed at room temperature.

2.10. Statistical analysis of data

Results are expressed as the mean ± SD. Multiple comparisons of means (one-way ANOVA) were used to substantiate statistical differences between groups, while Student's t-test was used to compare two samples. Data analysis was carried out with the software package XLStatistic for Microsoft Excel. Significance was tested at 0.05 level of probability (p).

3. Results and Discussion

3.1. Preparation and characterization of nanosuspension

A preliminary study was carried out to optimize the protocol for the CUR-NS preparation through the wet ball media milling technique. Two parameters were investigated, namely the stabilizer concentration and the milling time. CUR concentration was fixed at 1% (w/w), whereas two concentrations of the stabiliser P188 were studied: 0.5 and 1 % (w/w). The two formulations were milled for 60, 70, 80, and 90 minutes. Average diameter, PDI and zeta potential as a function of the milling time are shown in **Errore. L'origine r iferimento non è stata trovata.** for the formulation with 0.5% P188 and in **Errore. L'origine riferimento non è stata trovata.** for the one with 1% P188.

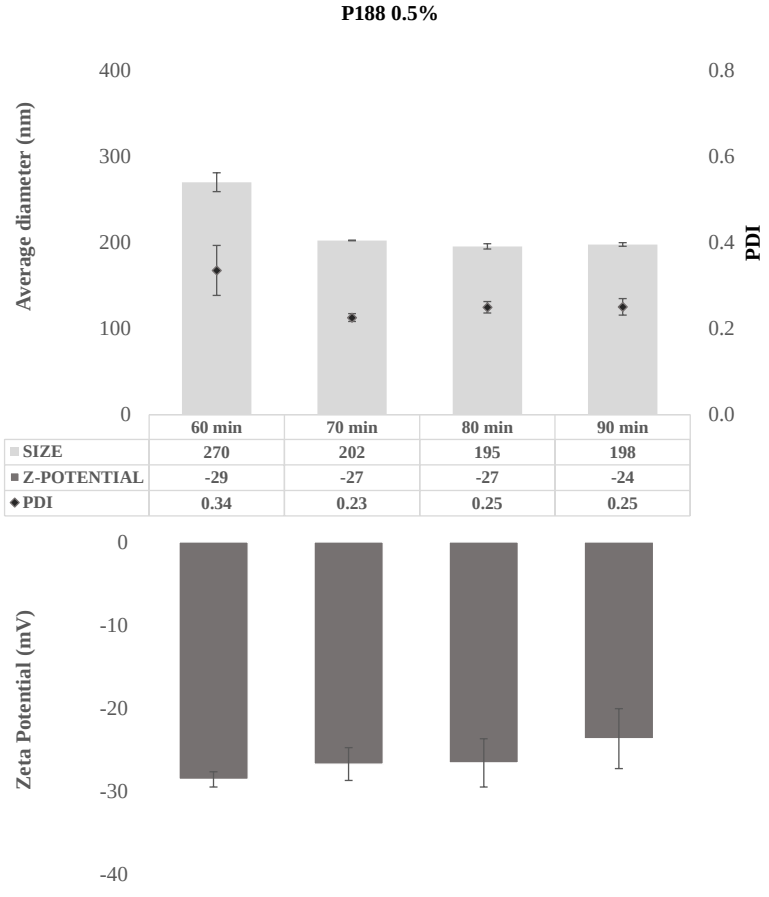

Figure 1. Average diameter (nm), PDI and Zeta Potential (mV) as a function of milling time (minutes) for the formulation with 1% (w/w) CUR and 0.5% (w/w) P188. (n=3; mean ± SD).

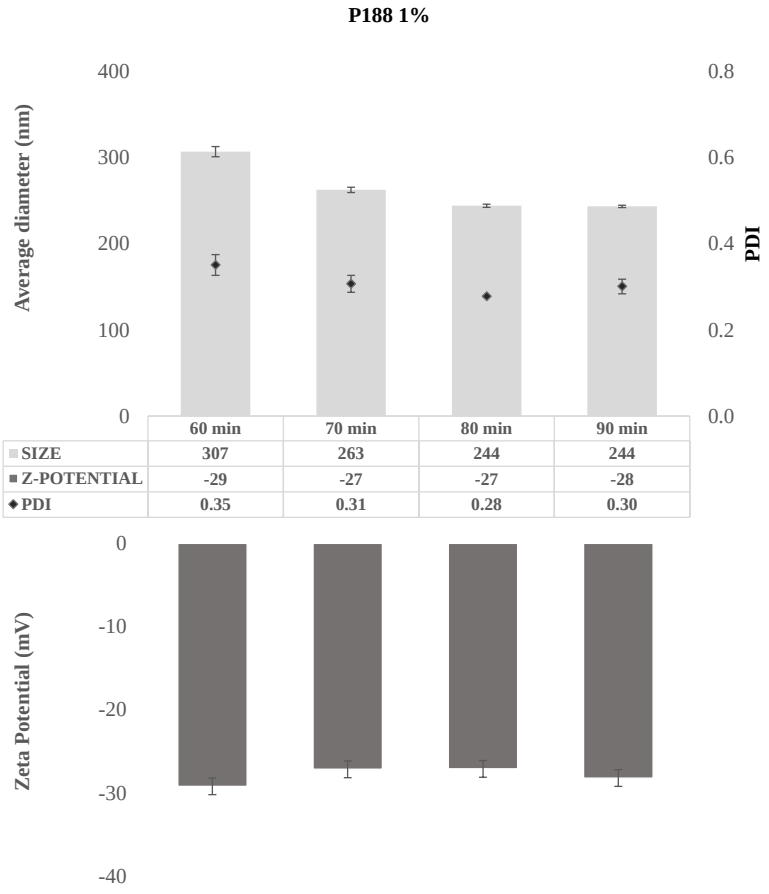

Figure 2. Average diameter (nm), PDI and Zeta Potential (mV) as a function of milling time (minutes) for the formulation with 1% (w/w) CUR and 1% (w/w) P188. (n=3; mean ± SD).

Both formulations showed a significant decrease in the nanocrystal average diameter by increasing the milling time from 60 to 70 minutes. As highlighted in Figure 1, also the PDI value improved for formulation with 0.5% P188, decreasing from 0.34 to 0.23. On the other hand, by increasing the milling time from 70 to 90 minutes, the variation of the nanocrystal dimensional properties was less pronounced. It is worth to notice that after all the milling protocols, the zeta potential values were maintained at approximately -30 mV, representative of promising formulation stability. However, as can be seen in the Figure 2, when the 1:1 drug:surfactant ratio (w/w) was used, the PDI never decreased to values less than approximately 0.30, even after 90 minutes of milling. Therefore, the formulation containing 1% CUR and 0.5% P188 obtained after 70 minutes of milling (CUR-NS) was selected for further studies.

CUR solubility studies were performed in water at 37 °C to evaluate the properties of nanocrystal CUR-NS in comparison with CUR raw powder. The raw drug powder showed a saturation solubility of 0.97 ± 0.1 μg/mL, whereas the nanocrystals, obtained after the milling procedure, reached a solubility value of 53.08 ± 1.7 μg/mL. Consequently, preparation of nanocrystals stabilised by P188, allowed us to improve CUR solubility by approximately 54-folds in comparison with the raw material, in accordance with the Freundlich-Ostwald equation [15].

The evaluation of the morphological changes of CUR crystals after the milling process was carried out by ESEM (**Errore. L'origine riferimento non è stata trovata.**).

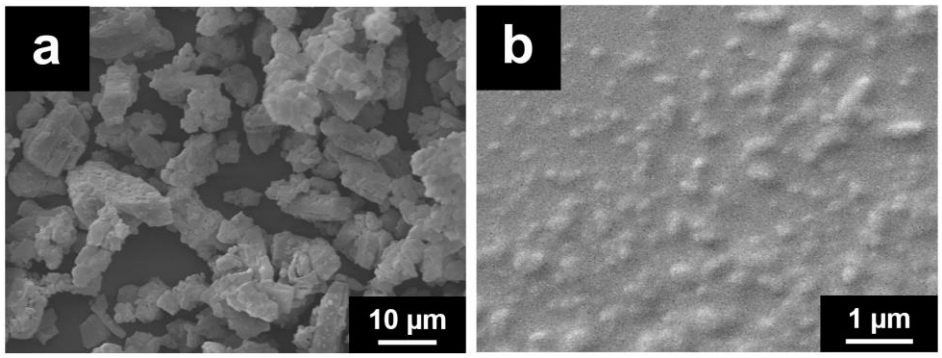

Figure 3. ESEM micrographs of CUR raw powder (a) and CUR-NS (b).

As it can be seen in the ESEM micrographs, the milling process modified both shape and size of the CUR crystals. The considerable amount of energy required to reduce the nanocrystal size below one micron is provided during the milling process by the collision of the drug crystals and the milling beads – and of the drug crystals themselves – that generate high shear forces. Before the milling, Figure 3a, the raw drug material appears to have large crystals with irregular elongated shape while, after the milling with the stabilizer, as shown in Figure 3b, CUR nanocrystals show a regular and rounded shape, with a homogenous particle size distribution, in accordance with DLS analysis.

The stability of the obtained CUR-NS was evaluated by monitoring size distribution and zeta-potential over a period of 90 days at room temperature (Figure 4).

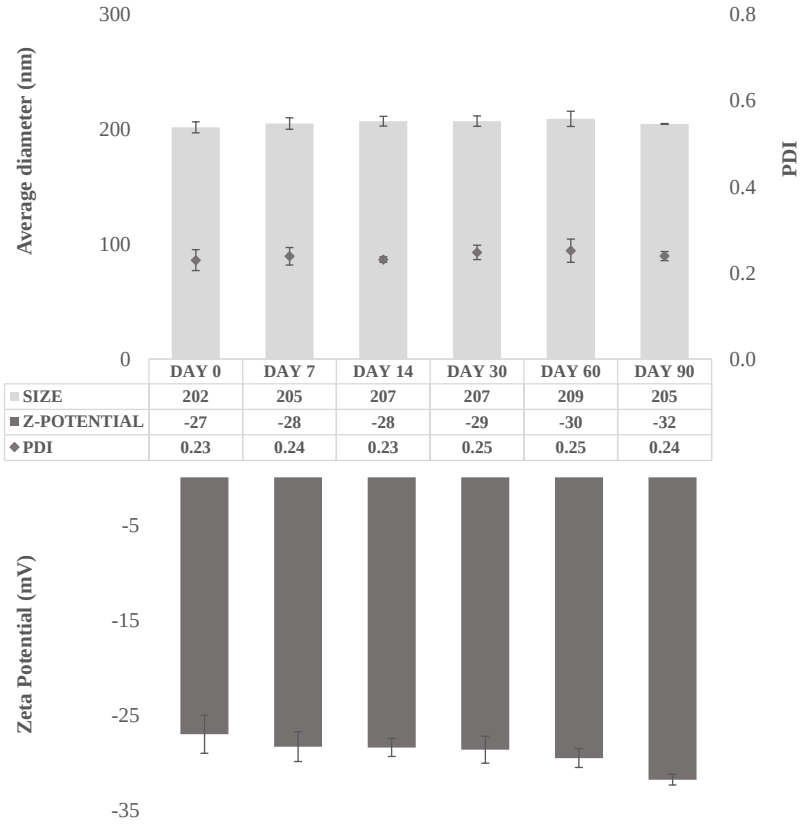

Figure 4. Average diameter (nm), polydispersity index (PDI) and Zeta Potential (mV) of CUR-NS over 90 days of storage at room temperature. (n=5; mean ± SD).

Size distribution study revealed a long-term stability of the CUR-NS. Indeed, the mean diameter did not vary appreciably during the 90 days on storage showing an average diameter of 202 nm in the day 1 and of 205 nm in day 90. Furthermore, the PDI was almost constant and below 0.25, confirming the stability of the formulation since the retention of the homogeneous size distribution on storage [28]. Moreover, the zeta potential value was almost constant during the stability test (approximately -30 mV).

The final multicomponent nanosuspension (CUR+BDP-NS) was obtained by mixing CUR-NS with BDP-NS, which was prepared according to the previously reported procedure [21] with a 1% (w/w) BDP concentration and 0.5% (w/w) P188. BDP nanocrystals exhibited a mean diameter of approximately 240 nm, with a low PDI (0.24) indicating a well-dispersed colloidal dispersion.

Solid state characterization of CUR-NS, BDP-NS and their components as raw material and physical mixture was carried out by ATR-FTIR, DSC and XRPD.

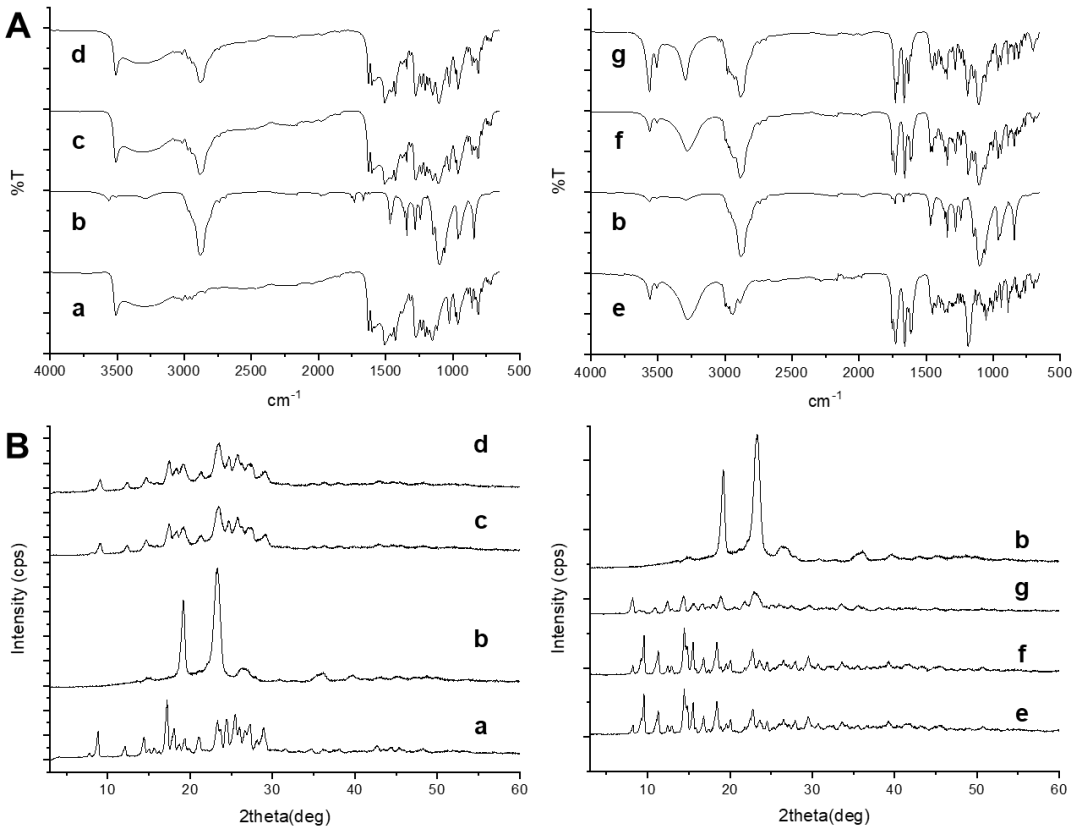

Figure 5. ATR-FTIR (A) and XRPD (B) analysis of CUR raw powder (a), P188 (b). physical mixture of CUR+P188 (c), CUR-NS (d), BDP raw powder (e), physical mixture of BDP+P188 (f) and BDP-NS (g).

To evaluate the possible interactions between CUR and the stabilizer in the preparation, thermal analysis was performed; results are expressed as onset temperature. CUR thermogram (not shown) revealed the presence of an endothermic peak at 165.05 °C, while P188 at 53.71°C, which implies that both are in the crystalline state. In the physical mixture, both the sharp endothermic peak of the stabilizer and the broad CUR peak, showed less intensity and a shift towards lower temperatures, (47.96 °C and 147.35 °C, respectively) compared to the component melting points, suggesting a molecular dispersion of CUR in P188. This trend became even more evident in the optimized formulation, thus, suggesting that the CUR existed in a less crystalline state. ATR spectroscopy (Figure 5A) was carried out to further elucidate the interactions between CUR and P188 in the solid

state. These interactions are detected by any changes in the position or disappearance of a characteristic vibration or stretching region of the compounds. The ATR spectrum of CUR exhibited a sharp peak at 3509 and a broad one at 3326 cm-1 attributed to phenolic OH stretching. Furthermore, it can be observed a peak at 1626 cm-1 owing to the carbonyl in CUR, consistent with the formation of a keto-enol tautomer, at 1602 and 1510 cm-1 the bands of the strong vibrations of C==C and C=O stretching, while at 1274 cm-1 the C- O peak of enol. At 1027 cm-1 the C -O- C peak was visible, while at 962 cm-1 and 810 cm-1 the trans-C-H vibration of the unsaturated chain and the C-H vibration of aromatic ring, respectively, were clearly showed. Finally, the characteristic absorption peaks of P188 around 3600, 2881, and 1099 cm−1 were attributed to O-H, C–H, and C–O–C stretching vibrations. The spectrum of the physical mixture was the combination of CUR and P188. These results clearly demonstrated that no interactions occurred between the physically mixed CUR and P188. The spectra of CUR-NS exhibited the same peak position of raw CUR demonstrating that the addition of the stabilizer and physical process would not affect its molecular structure.

The CUR crystalline state in nanosuspension was estimated by a XRPD study (Figure 5B). The diffraction patterns of CUR showed intense sharp peaks at 8.8, 12.1, 14.4, 17.2, 18.08, 19.36, 21.08, 21.66, 23.32, 24.46, 25.48, 27.28 and 28.10 2ϑ (deg), while P188 at 19.32 and 23.48 2ϑ (deg) implying the crystalline structure of the both raw materials. The physical mixture and the nanosupension profiles were very similar; reflection peaks of the raw materials were still present indicating that CUR partially retained its crystallinity in the formulation.

As it concerns BDP-NS and its components, the BDP thermal behaviour (thermogram not shown) revealed an endothermic peak at 212.09 °C (onset temperature) followed by an exothermic event, thus, indicating that the recrystallized BDP undergoes a melting process followed by chemical degradation.

The melting peak of P188 was at an onset temperature of 53.71 °C. Physical mixture and nanosuspension thermograms showed some similarities, in fact, the melting peaks were all present but drifted, and with a sharp decrease in the BDP peak intensity, implying that no amorphous forms were produced during the preparation process. The ATR spectrum of BDP (Figure 5A) showed the O-H free and associated vibrations at 3559 and 3280 cm-1, the ester carbonyl stretching at 1753, the conjugated and non-conjugated C=O stretching bands at 1727 and 1658 cm-1, respectively. The C=C stretching was at 1615 and 1608 cm-1, and the C-O bands at 1186 cm-1. The characteristic absorption peaks of P188 at 3500, 2881, and 1099 cm−1 were attributed to O-H, C–H, and C–O–C stretching vibrations, respectively. In the physical mixture spectrum, bands of both raw materials were visible, no absence of any functional peaks or addition of new peaks, thus, revealing that there is no significant chemical interaction between the drug and P188. In the nanosuspension spectrum, as reported in our previous article [21], the COO peak, the C=O and C=C stretchings at 1711, 1663 and 1631 respectively disappeared while a peak at 1712 cm-1 appeared, suggesting that the BDP carbonyl group is involved in a hydrogen bond with water. The presence of water was also confirmed by the increase of peak intensities at 3562 and 3508 cm^{-1}, suggesting the presence of BDP as monohydrate. To confirm the crystalline nature of BDP nanosuspension, X-ray diffraction analysis were performed (Figure 5B). BDP and P188 have crystalline profiles. The XRPD analysis of BDP showed a pattern with sharp and intense peaks at 9.54, 11.28, 14.44 and 20.06 2θ (deg) values, P188 at 19.32 and 23.48 2ϑ (deg). The physical mixture pattern indicated that the crystalline structure remained unchanged; the characteristic peaks of the drug were still present, even if their intensities were attenuated due to the lower drug content. The optimized NS retained the crystalline profile, but the increased intensity of the peaks at 8.5° and 12 2ϑ (deg) suggested the presence of BDP monohydrate, thus supporting ATR results.

3.2. Preparation of the multicomponent nanosuspension

After the optimization and characterization of the two single-component nanosuspensions, CUR+BDP-NS was prepared by mixing equal amounts of CUR-NS and BDP-NS right before the nebulization test. The composition of the obtained formulation is indicated in the **Errore. L'origine riferimento non è stata trovata.**. A preliminary visual inspection revealed the absence of macroscopic precipitated aggregates or phase separation. This information was also confirmed by DLS analysis. Indeed, the nanocrystals average diameter of the CUR+BDP-NS (221nm) did not differ appreciably from CUR-NS (202 nm) and BDP-NS (241 nm.) Furthermore, the PDI maintained a value of approximately 0.25.

Table 1. Composition of the two single-component (CUR-NS, BDP-NS) and the multicomponent formulation (CUR+BDP-NS) and their dimensional properties expressed as average diameter (nm) and polydispersity index (PDI). (n=3; mean ± SD).

	Composition			**Dimensional Analysis**	
	Curcumin (% w/w)	Beclomethasone dipropionate (% w/w)	P188 (% w/w)	Average diameter (nm)	PDI
CUR-NS	1	-	0.5	202 ± 5	0.23 ± 0.02
BDP-NS	-	1	0.5	241 ± 2	0.24 ± 0.01
CUR+BDP-NS	0.5	0.5	0.5	221 ± 7	0.25 ± 0.02

3.2. Nebulization test

To evaluate the drug deposition and determine the aerodynamic parameters, samples (CUR-NS, BDP-NS, CUR+BDP-NS) were nebulized using the PariSX® air jet nebulizer connected to the NGI. It is well known that nebulizers might generate aerosol particles with different aerodynamic diameters. In particular, only those characterized by a MMAD value in the range 5 – 0.5 μm are believed to deposit on the lungs [29]. Operating with a flow rate of 15 L/min, the overall range of the impactor is 0.98–14.1 μm. Notably, four stages have cut sizes in the range of 0.5–5.0 μm aerodynamic diameter, and a fifth stage only slightly larger than the upper limit [26]. Nebulization time to dryness, which is the time required to complete cessation of aerosol formation, was shown to be 10 minutes. The percentage of drug deposited in each stage of the impactor was very similar for all the formulations, as shown in the **Errore. L'origine riferimento non è stata trovata.**6.

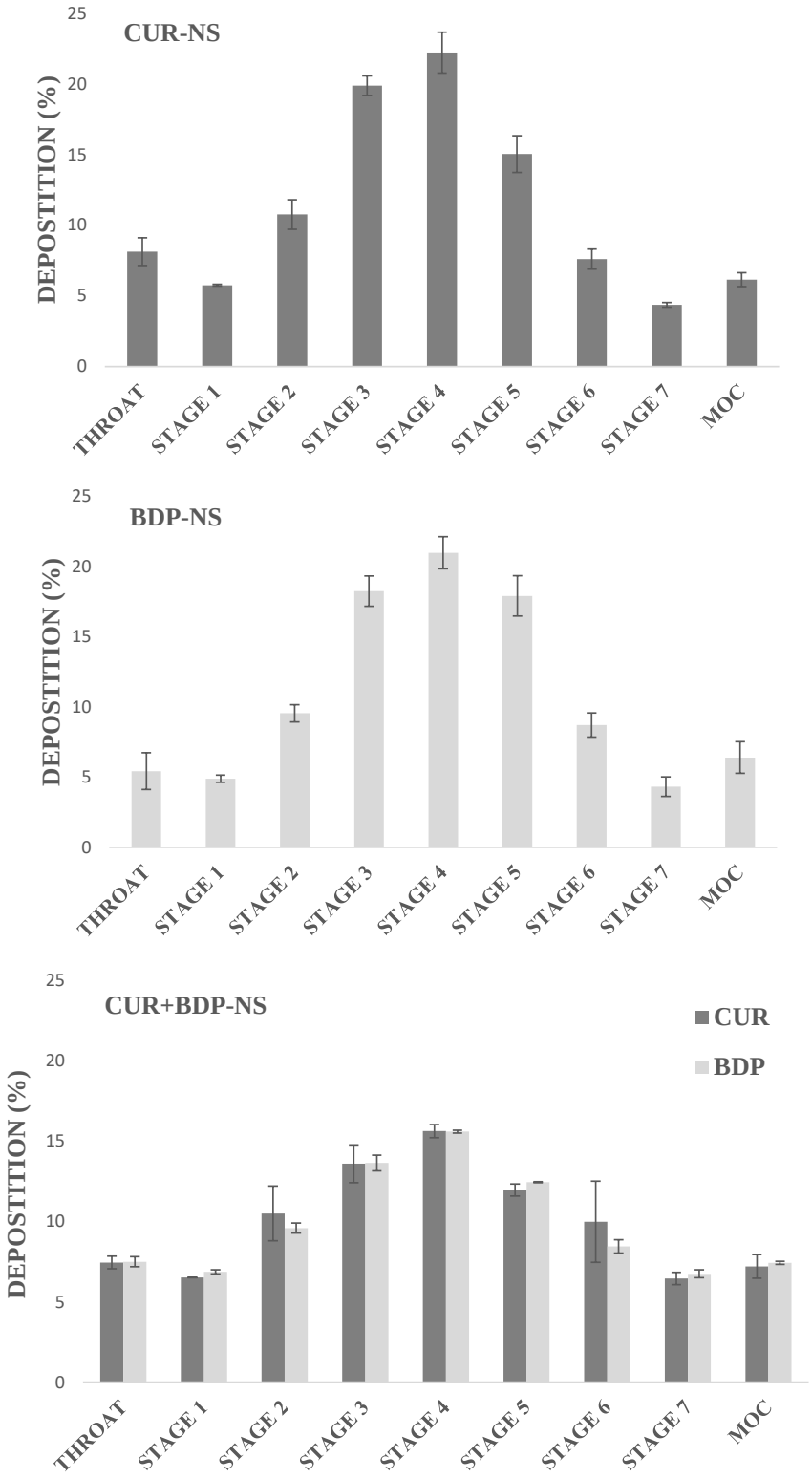

Figure 6. Deposition of CUR and BDP in the different stages of the NGI after nebulization with a flow rate of 15 L/min, for the single-component formulations (CUR-NS and BDP-NS), and the multicomponent formulation (CUR+BDP-NS). (n=3; mean ± SD).

Approximately 5 – 7% of the generated aerosol particles tend to deposit on the induction port (throat), thus showing their inhability to reach the deeper stages. However, the majority of the drug was found to be in the intermediate/middle stages (3 – 5). Interestingly, approximately 6-7% of the droples is able to reach the MOC stage, showing an aerodynamic diameter < 0.98 μm, and thus the ability to hypothetically deposit on the alveolar region of the lungs. To better evaluate the nanosuspension behaviour during the nebulization process, the aerodynamic parameters were analysed for each formulation (**Errore. L'origine riferimento non è stata trovata.**). In the case of CUR+BDP-NS, values w ere calculated separately for each active ingredient.

Table 2. Aerodynamic parameters of the three tested formulations: Emitted dose (ED), Fine Particle Dose (FPD), Fine Particle Fraction (FPF), Mass Median Aerodinamic Diameter (MMAD) and Geometric Standard Deviation (GSD). (n=3; mean ± SD).*Data are not statistically different (p>0.05).

		CUR+BDP-NS		
	CUR-NS	**CUR**	**BDP**	**BDP-NS**
ED%	57.0 ± 0.9	81.9 ± 1.1	83.4 ± 3.7	65.5 ± 4.9
FPD (mg)	7.8 ± 0.3	6.8 ± 0.8	6.1 ± 0.1	7.6 ± 0.2
FPF (%)	60.3 ± 1.9 *	64.7 ± 4.0 *	62.7 ± 0.5 *	68.1 ± 7.2 *
MMAD (μm)	4.1 ± 0.1	3.4 ± 0.6	3.8 ± 0.1	3.7 ± 0.2
GSD	2.6 ± 0.1	3.1 ± 0.4	2.9 ± 0.1	2.6 ± 0.1

As can be seen, the Emitted Dose (ED) for CUR-NS and BDP-NS reached a value of 57% and 65.5%., respectively. It is interesting to highlight that this value increases more than 80% in the case of the multicomponent formulation, thus, demonstrating that more than 80% of the formulation loaded in the nebulizer may be properly delivered to the patient. This result might be explained by a stabilization of the two active ingredients when combined together, leading to an improved nebulization. Results showed that the mean FPF% value for the CUR in the multicomponent nanosuspension was higher than that in the CUR-NS whilethe opposite was for the BDP. However, statistical analysis revealed that these differences are not significative (p>0.05).

Finally, all the nebulized formulations showed a MMAD <5 μm, a mandatory condition for the droplets to be able to reach the deeper parts of the respiratory system, and therefore to carry out their therapeutic action at the site of inflammation.

4. Conclusion

In this study, a CUR nanosuspension was optimized and characterized. The resulting nanocrystals were small in size and homogeneously dispersed, showing an increased solubility compared to the bulk drug. Furthermore, the BDP-NS was successfully prepared as reported previously [24], and used for the preparation of the multicomponent nanosuspension, containing CUR and BDP nanocrystals. The obtained formulation showed a narrow distribution and the absence of aggregation phenomena. In vitro nebulization tests were carried out and highlighted that all prepared formulations, especially CUR+BDP-NS, had high values of ED% and MMAD < 5 μm.

In conclusion, the obtained multicomponent nanosuspension has shown optimal dimensional properties and aerodynamic parameters, suggesting a correct and efficient delivery of the formulation in the deeper lung regions.

Owing to the improved solubility of the active ingredients formulated as nanocrystals, our formulation represents a promising lung delivery system which can improve the course of the asthmatic inflammation.

Author Contributions: Conceptualization, A.M.F., F.L.; Data curation, L.C., Formal analysis, L.C., C.S., M.C.C.,S.M.; Investigation, D.V., L.C., E.P., G.A., M.C.C.; Methodology, D.V., L.C., E.P., S.M.; Resources, A.M.F. ; Supervision, A.M.F., C.S. ; Validation, F.L., L.C. ; Visualization, F.L., L.C.; Writing – original draft, L.C.; Writing – review & editing, A.M.F., C.S.

Funding: This work was supported by UniCA-Progetti biennali di Ateneo Finanziati dalla Fondazione di Sardegna 2018 (CUP F74I19000950007).

Conflicts of Interest: The authors declare no conflict of interest.

References

1. Carr, T.F.; Bleecker, E. Asthma heterogeneity and severity. *World Allergy Organ. J.* **2016**, *9*, 41.
2. Nakagome, K.; Nagata, M. Pathogenesis of airway inflammation in bronchial asthma. *Auris Nasus Larynx* **2011**, *38*, 555–563.
3. Kuruvilla, M.E.; Lee, F.E.H.; Lee, G.B. Understanding Asthma Phenotypes, Endotypes, and Mechanisms of Disease. *Clin. Rev. Allergy Immunol.* **2019**, *56*, 219–233.
4. Wenzel, S.E. Asthma phenotypes: the evolution from clinical to molecular approaches. *Nat. Med.* **2012**, doi:10.1038/nm.2678.
5. Christman, J.W.; Sadikot, R.T.; Blackwell, T.S. The role of nuclear factor-κ B in pulmonary diseases. *Chest* **2000**, *117*, 1482–1487, doi:10.1378/chest.117.5.1482.
6. Global Initiative for Asthma *Global strategy for asthma management and prevention.*; **2020**;
7. Park, H.S.; Kim, S.R.; Kim, J.O.; Lee, Y.C. The roles of phytochemicals in bronchial asthma. *Molecules* **2010**, *15*, 6810–6834, doi:10.3390/molecules15106810.
8. Abidi, A.; Gupta, S.; Agarwal, M.; Bhalla, H.L.; Saluja, M. Evaluation of efficacy of curcumin as an add-on therapy in patients of bronchial asthma. *J. Clin. Diagnostic Res.* **2014**, *8*, HC19, doi:10.7860/JCDR/2014/9273.4705.
9. Oh, S.W.; Cha, J.Y.; Jung, J.E.; Chang, B.C.; Kwon, H.J.; Lee, B.R.; Kim, D.Y. Curcumin attenuates allergic airway inflammation and hyper-responsiveness in mice through NF-κB inhibition. *J. Ethnopharmacol.* **2011**, *136*, 414–421, doi:10.1016/j.jep.2010.07.026.
10. Chong, L.; Zhang, W.; Nie, Y.; Yu, G.; Liu, L.; Lin, L.; Wen, S.; Zhu, L.; Li, C. Protective Effect of Curcumin on Acute Airway Inflammation of Allergic Asthma in Mice Through Notch1–GATA3 Signaling Pathway. *Inflammation* **2014**, *37*, 1476–1485, doi:10.1007/s10753-014-9873-6.
11. Shahid, H.; Shahzad, M.; Shabbir, A.; Saghir, G. Immunomodulatory and Anti-Inflammatory Potential of Curcumin for the Treatment of Allergic Asthma: Effects on Expression Levels of Pro-inflammatory Cytokines and Aquaporins. *Inflammation* **2019**, *42*, 2037–2047, doi:10.1007/s10753-019-01066-2.
12. Lai, F.; Schlich, M.; Pireddu, R.; Fadda, A.M.; Sinico, C. Nanocrystals as Effective Delivery Systems of Poorly Water-soluble Natural Molecules. *Curr. Med. Chem.* **2018**, *26*, 4657–4680, doi:10.2174/0929867326666181213095809.
13. Lai, F.; Schlich, M.; Pireddu, R.; Corrias, F.; Fadda, A.; Sinico, C. Production of nanosuspensions as a tool to improve drug bioavailability: focus on topical delivery. *Curr. Pharm. Des.* **2015**, *21*, 6089–6103, doi:10.2174/1381612821666151027152350.
14. Mosharraf, M.; Nyström, C. The effect of particle size and shape on the surface specific dissolution rate of microsized practically insoluble drugs. *Int. J. Pharm.* **1995**, *122*, 35–47, doi:10.1016/0378-5173(95)00033-F.
15. Müller, R.H.; Peters, K. Nanosuspensions for the formulation of poorly soluble drugs. I. Preparation by a size-reduction technique. *Int. J. Pharm.* **1998**, *160*, 229–237, doi:10.1016/S0378-5173(97)00311-6.
16. Jacobs, C.; Müller, R.H. Production and characterization of a budesonide nanosuspension for pulmonary administration. *Pharm. Res.* **2002**, *19*, 189–194, doi:10.1023/A:1014276917363.

17. Chiang, P.C.; Alsup, J.W.; Lai, Y.; Hu, Y.; Heyde, B.R.; Tung, D. Evaluation of aerosol delivery of nanosuspension for pre-clinical pulmonary drug delivery. *Nanoscale Res. Lett.* **2009**, *4*, 254–261, doi:10.1007/s11671-008-9234-1.
18. Zhang, Y.; Zhang, J. Preparation of budesonide nanosuspensions for pulmonary delivery: Characterization, in vitro release and in vivo lung distribution studies. *Artif. Cells, Nanomedicine Biotechnol.* **2016**, *44*, 285–289, doi:10.3109/21691401.2014.944645.
19. Van Eerdenbrugh, B.; Van den Mooter, G.; Augustijns, P. Top-down production of drug nanocrystals: Nanosuspension stabilization, miniaturization and transformation into solid products. *Int. J. Pharm.* **2008**, *364*, 64–75.
20. Britland, S.; Finter, W.; Chrystyn, H.; Eagland, D.; Abdelrahim, M.E. Droplet aerodynamics, cellular uptake, and efficacy of a nebulizable corticosteroid nanosuspension are superior to a micronized dosage form. *Biotechnol. Prog.* **2012**, *28*, 1152–1159, doi:10.1002/btpr.1616.
21. Yang, J.Z.; Young, A.L.; Chiang, P.C.; Thurston, A.; Pretzer, D.K. Fluticasone and budesonide nanosuspensions for pulmonary delivery: Preparation, characterization, and pharmacokinetic studies. *J. Pharm. Sci.* **2008**, *97*, 4869–4878, doi:10.1002/jps.21380.
22. Dompeling, E.; van Schayck, C.P.; Molema, J.; Folgering, H.; van Grunsven, P.M.; van Weel, C. Inhaled beclomethasone improves the course of asthma and COPD. *Eur. Respir. J.* **1992**, *5*, 945–52.
23. Corrias, F.; Schlich, M.; Sinico, C.; Pireddu, R.; Valenti, D.; Fadda, A.M.; Marceddu, S.; Lai, F. Nile red nanosuspensions as investigative model to study the follicular targeting of drug nanocrystals. *Int. J. Pharm.* **2017**, *524*, 1–8, doi:10.1016/j.ijpharm.2017.03.042.
24. Casula, L.; Sinico, C.; Valenti, D.; Pini, E.; Pireddu, R.; Schlich, M.; Lai, F.; Maria Fadda, A. Delivery of beclomethasone dipropionate nanosuspensions with an electronic cigarette. *Int. J. Pharm.* **2021**, *596*, doi:10.1016/j.ijpharm.2021.120293.
25. Berg, E.; Lamb, P.; Ali, A.; Dennis, J.; Tservistas, M.; Mitchell, J. Assessment of the need to coat particle collection cups of the NGI to mitigate droplet bounce when evaluating nebuliser-produced droplets. *Pharmeur. Sci. Notes* **2008**, *2008*, 21–25.
26. Marple, V.; Santhanakrishnan, K.; Mitchell, J.P.; Roberts, D.L.; Hudson-curtis, B.L. Next Generation Pharmaceutical Impactor: A New Impactor for Pharmaceutical Inhaler Testing. Part III. Extension of Archival Calibration to 15 L/min. *J. Aerosol Med.* **2004**, *17*, 335–343.
27. Manca, M.L.; Peris, J.E.; Melis, V.; Valenti, D.; Cardia, M.C.; Lattuada, D.; Escribano-Ferrer, E.; Fadda, A.M.; Manconi, M. Nanoincorporation of curcumin in polymer-glycerosomes and evaluation of their in vitro-in vivo suitability as pulmonary delivery systems. *RSC Adv.* **2015**, *5*, 105149–105159, doi:10.1039/c5ra24032h.
28. Patravale, V.B.; Date, A.A.; Kulkarni, R.M. Nanosuspensions: a promising drug delivery strategy. *J. Pharm. Pharmacol.* **2004**, *56*, 827–840, doi:10.1211/0022357023691.
29. Yang, W.; Peters, J.I.; Williams, R.O. Inhaled nanoparticles-A current review. *Int. J. Pharm.* 2008, *356*, 239–247.